

## 1E 1207.4–5209: THE PUZZLING PULSAR AT THE CENTER OF THE PKS 1209–51/52 SUPERNOVA REMNANT

G. G. PAVLOV<sup>1</sup>, V. E. ZAVLIN<sup>2</sup>, D. SANWAL<sup>1</sup>, AND J. TRÜMPER<sup>2</sup>

## ABSTRACT

Second *Chandra* observation of 1E 1207.4–5209, the central source of the supernova remnant PKS 1209–51/52, allowed us to confirm the previously detected period of 424 ms and, assuming a uniform spin-down, estimate the period derivative,  $\dot{P} \sim (0.7\text{--}3) \times 10^{-14} \text{ s s}^{-1}$ . The corresponding characteristic age of the pulsar,  $P/2\dot{P} \sim 200\text{--}900 \text{ kyr}$ , is much larger than the estimated age of the SNR,  $\sim 7 \text{ kyr}$ . The values of the spin-down luminosity,  $\dot{E} \sim (0.4\text{--}1.6) \times 10^{34} \text{ erg s}^{-1}$ , and conventional magnetic field,  $B \sim (2\text{--}4) \times 10^{12} \text{ G}$ , are typical for a middle-aged radio pulsar, although no manifestations of pulsar activity have been observed. If 1E 1207.4–5209 is indeed the neutron star formed in the same supernova explosion that created PKS 1209–51/52, such a discrepancy in ages could be explained either by a long initial period, close to its current value, or, less likely, by a very large braking index of the pulsar. Alternatively, the pulsar could be a foreground object unrelated to the supernova remnant, but the probability of such a coincidence is very low.

*Subject headings:* pulsars: individual (1E 1207.4–5209) — stars: neutron — supernovae: individual (PKS 1209–51/52) — X-rays: stars

## 1. INTRODUCTION

Radio-quiet compact central objects of supernova remnants (SNRs) have emerged recently as a separate class of X-ray sources (see, e.g., Pavlov et al. 2002, for a review). The nature of at least some of these sources, presumably neutron stars (NSs), remains enigmatic. They are characterized by soft, apparently thermal, X-ray spectra and a lack of observed pulsar activity and optical counterparts. One of the most important properties, which potentially allows one to elucidate the nature of these sources, is the periodicity of their radiation. Our previous observation of 1E 1207.4–5209, the central object of PKS 1209–51/52 (=G296.5+10.0), with the Advanced CCD Imaging Spectrometer (ACIS) on board of the *Chandra* X-ray observatory allowed us to detect a period  $P = 0.424129 \text{ s}$  (Zavlin et al. 2000; Paper I hereafter), which proved that the source is indeed a neutron star. This source was discovered with the *Einstein* observatory (Helfand & Becker 1984), 6' off the center of the 81' diameter SNR. From the analysis of radio and optical observations of this SNR, Roger et al. (1988) estimated the SNR age to be 7 kyr, with an uncertainty of a factor of 3. The distance to the SNR is  $d = 2.1_{-0.8}^{+1.8} \text{ kpc}$  (Giacani et al. 2000). The X-ray spectrum of the central source can be described by a thermal model, with a blackbody temperature of 3–4 MK and a radius of 1–2 km, at  $d = 2 \text{ kpc}$  (Mereghetti, Bignami, & Caraveo 1996; Vasisht et al. 1997; Zavlin, Pavlov, & Trümper 1998). Fitting the spectrum with a hydrogen atmosphere model, Zavlin et al. (1998) obtained an effective temperature of 1.4–1.9 MK and a radius of about 10–12 km. Mereghetti et al. (1996) reported upper limits on the source flux in radio ( $< 0.1 \text{ mJy}$  at 4.8 GHz), optical ( $V > 23.5$ ), and  $\gamma$ -rays ( $< 1 \times 10^{-7} \text{ photons cm}^{-2} \text{ s}^{-1}$  for  $E > 100 \text{ MeV}$ ).

In this Letter we present the results of second *Chandra* ACIS observation, which allowed us to estimate the period derivative and other parameters of the pulsar.

## 2. OBSERVATION AND DATA REDUCTION

1E 1207.4–5209 was observed with *Chandra* on 2002 January 5–6 with the spectroscopic array ACIS-S in the Continuous Clocking (CC) mode. This mode provides the highest time

resolution of 2.85 ms available with ACIS at the expense of one dimension of image. The source was imaged on the back-illuminated chip S3, at a focal plane temperature of  $-120 \text{ C}$ . The total duration of the observation was 31.6 ks. Time history of detected events does not reveal substantial background flares, so we do not exclude any time intervals from the analysis.

The 1D image of 1E 1207.4–5209 in “sky pixels” is consistent with the ACIS Point Spread Function, and it is similar to the image obtained in the previous observation, taken at almost the same roll angle of  $65.2^\circ$  (vs.  $65.3^\circ$  in the second observation). To obtain the source count rate, we extracted 20,282 source-plus-background counts from a 1D segment of 8 pixel length centered at the source position (10 pixels contain 20,588 counts). The background was taken from similar segments adjacent to the 1D source aperture. Subtracting the background, we find a source countrate of  $0.64 \pm 0.01 \text{ s}^{-1}$ , versus  $0.76 \pm 0.01 \text{ s}^{-1}$  in the previous ACIS observation. The reduction of the count rate can be attributed to a reduction of ACIS sensitivity at low energies.

## 3. TIMING ANALYSIS

The event times in the event file of a CC observation are the times when the event is read out at the chip node. To restore the actual event arrival times, we subtracted the times of charge transfer between the detection point and the readout node from the readout times and corrected the times for the satellite wobbling (dither) and the Science Instrument Module motion using the approach described in Paper I. The corrected times were transformed to the solar system barycenter using the `axBary` tool of the CIAO package (v. 2.2).

From a 3-pixel segment centered at the source position, we extracted 18,237 counts in the 0.3–4.0 keV energy range, where the background contribution is negligible (about 0.7%). We ran the  $Z_m^2$  test ( $m$  is the number of harmonics included — see Buccheri et al. 1983) in the vicinity of the pulsation frequency determined in our previous observation. For  $m = 1, 2, 3, 4$ , and 5, we found the  $Z_m^2$  peak values of 62.2, 63.9, 73.0, 77.6, and 79.3 at frequencies lower than a reference frequency 2.35777 Hz by 5.2, 4.9, 2.4, 2.8, and 3.3  $\mu\text{Hz}$ , respectively. The probability to find such high peaks in a noise spectrum is extremely

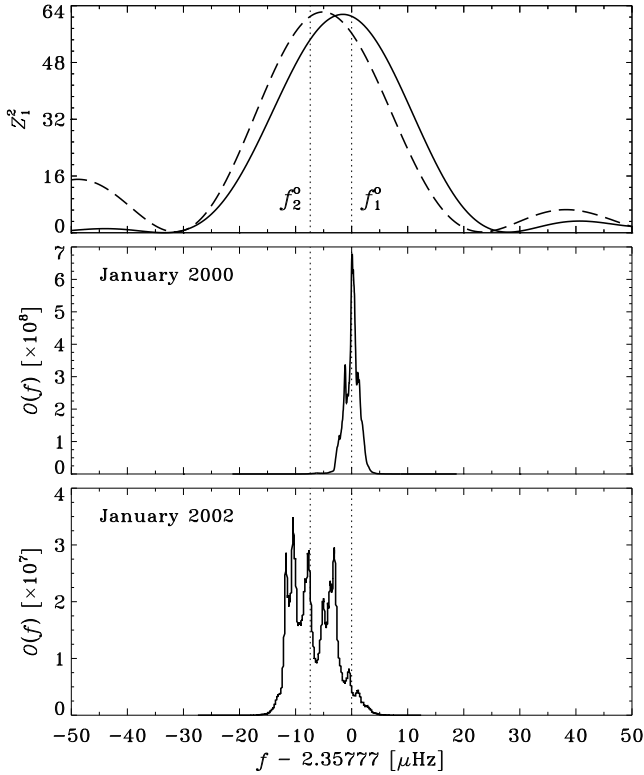


FIG. 1.— Power spectra (upper panel) and frequency dependences of odds ratio (middle and bottom panels) around the pulsation frequency for the first and second observations (solid and dashed curves in the upper panel, respectively). Dotted lines show the median frequencies  $f_{1,2}^0$  found in the two observations.

low,  $\sim 10^{-14}$  in a frequency range  $\lesssim 10 \mu\text{Hz}$ , which confirms our previous period detection. For a uniform comparison of the peak frequencies in first and second observations, we recalculated the  $Z_m^2$  peaks for the first observation using exactly the same extraction segments, energy range, and time corrections as in the second one and obtained  $Z_m^2 = 61.6, 61.8, 62.3, 62.7,$  and  $65.6$  (notice the smaller contributions from higher harmonics in first observation compared to second one, in which third and fourth harmonics are quite significant). The peak frequencies in the second observation are lower than in the first one:  $f_1 - f_2 = 4.2, 2.9, 1.1, 1.9,$  and  $2.2 \mu\text{Hz}$ , for  $m = 1, 2, 3, 4,$  and  $5$ , respectively. This result shows that the pulsar has slowed down in two years, although the scatter of the frequency shift is rather high.

To evaluate the most plausible frequencies and the frequency shift, we employed the method of Gregory & Loredó (1996), based on the Bayesian formalism. This method uses the phase-averaged epoch-folding algorithm to calculate the frequency-dependent odds ratio  $O(f)$ . This ratio specifies how the data favor a periodic model of a given frequency  $f$  over the unpulsed model, and it allows one to find the corresponding probability distribution  $p(f) \propto O(f) f^{-1}$  (see Gregory & Loredó 1996, Paper I, for details). The profile  $O(f)$  calculated for the second observation appears to be much broader than for the first one (FWHM  $\sim 10 \mu\text{Hz}$  vs.  $\sim 3 \mu\text{Hz}$ ), with several narrow peaks of comparable heights (see Fig. 1). Exploring the  $O(f)$  dependence in various energy ranges, which show different rel-

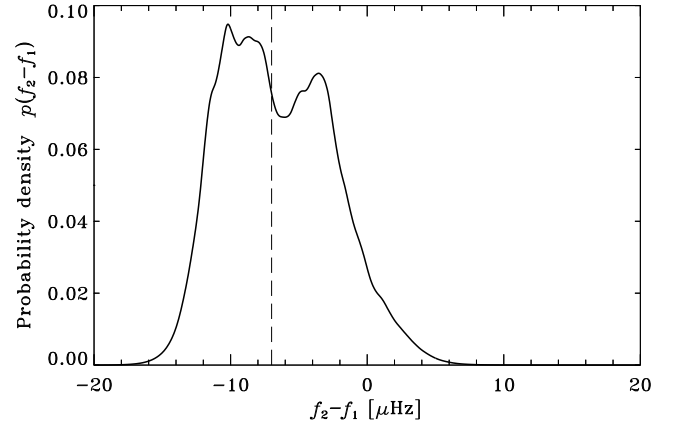


FIG. 2.— Probability distribution for the frequency shift (in  $\mu\text{Hz}^{-1}$ ). The vertical dash line shows the median shift.

ative contributions of the harmonics of the pulsation frequency, we found that the separate peaks are associated with different harmonics (e.g., the highest peak in the lower panel of Fig. 1 is associated with  $m = 1$ ), in agreement with the different  $Z_m^2$  peak frequencies mentioned above. The median frequency of the probability distribution in second observation, for the 0.3–4.0 keV band, is  $f_2^0 = 2.3577625 \text{ Hz}$ ; it differs from the mean frequency by  $\lesssim 0.1 \mu\text{Hz}$ . The uncertainties of the frequency are  $(-3.2, +4.5)$ ,  $(-4.2, +8.0)$ , and  $(-4.5, +10.1) \mu\text{Hz}$  at 68%, 90%, and 95% confidence level, respectively; the standard deviation is  $\sigma_{f_2} = 3.7 \mu\text{Hz}$ . We repeated a similar calculation for the data from the first observation (using the same extraction segment and energy range as for the second one) and obtained  $f_1^0 = 2.3577699 \text{ Hz}$ , with uncertainties of  $(-1.4, +1.2)$ ,  $(-2.5, +1.8)$ , and  $(-2.9, +2.1)$  at 68%, 90%, and 95% confidence level, respectively;  $\sigma_{f_1} = 1.3 \mu\text{Hz}$ .

We calculated the probability density distribution for the frequency difference,  $\Delta = f_2 - f_1$ , as  $p(\Delta) = \int p_2(f) p_1(f - \Delta) df$  (see Fig. 2), where  $p_1(f_1)$  and  $p_2(f_2)$  are the probability densities obtained for the two observations. The median of this distribution,  $\Delta^0 = -7.0 \mu\text{Hz}$ , gives a shift somewhat smaller than the mean shift,  $\int \Delta p(\Delta) d\Delta \simeq f_2^0 - f_1^0 = -7.4 \mu\text{Hz}$ , but the difference is well within the uncertainties of  $\Delta$ :  $(-3.8, +4.5)$ ,  $(-5.4, +7.1)$ , and  $(-5.9, +8.3) \mu\text{Hz}$  at 68%, 90%, and 95% confidence level, respectively;  $\sigma_\Delta = 3.9 \mu\text{Hz}$ . Because of the large widths of the  $p_2(f_2)$  and, consequently,  $p(\Delta)$  distributions, there is a non-negligible (albeit small) 5.6% probability that  $f_2 > f_1$ .

Adopting  $\Delta^0 = -7.0_{-3.8}^{+4.5} \mu\text{Hz}$  for the frequency shift and assuming a steady slowdown (lack of strong timing noise, glitches, etc) during two years between the observations, we obtain the following estimates for the time derivatives

$$\dot{f} = -1.1_{-0.6}^{+0.7} \times 10^{-13} \text{ Hz s}^{-1}, \quad \dot{P} = 2.0_{-1.3}^{+1.1} \times 10^{-14} \text{ s s}^{-1}. \quad (1)$$

The light curve extracted at  $f = f_2^0$  in the energy range 0.3–4.0 keV (Fig. 3, right panel) reveals one broad pulse per period with a source pulsed fraction of  $f_p = 8 \pm 2\%$ , similar to that obtained in first observation. Figure 3 indicates that in both observations there is a considerable shift of the pulse phase, up to 0.4–0.6, between the energy bands 0.3–1.0 and 1.0–1.7 keV, perhaps accompanied by a change of the pulse shape. (Similar behavior has been observed in a number of middle-aged pulsars

— e.g., Ögelman 1995.) There is also some evidence that the pulse shapes are different in the two observations — e.g., in the 0.3–4.0 keV band the pulse is closer to a sinusoid in first observation while its shape becomes more “triangular” in second observation.

#### 4. DISCUSSION

The detection of approximately the same period in the second observation confirms our previous detection and proves unambiguously that 1E 1207.4–5209 is a neutron star. However, the time derivative of the period appears to be surprisingly small — the corresponding characteristic age of the pulsar,  $\tau_c = P/(2\dot{P}) = 340_{-120}^{+600}$  kyr, exceeds the estimated SNR age, 3–20 kyr, by a large factor, and even the most conservative upper limit,  $\dot{P} < 5 \times 10^{-14}$  s s $^{-1}$ , yields an incredibly old age,  $\tau_c > 130$  kyr. Such values of  $P$  and  $\dot{P}$ , as well as the corresponding values of rotation energy loss rate,  $\dot{E} = 4\pi^2 I \dot{P} P^{-3} = 1.0_{-0.7}^{+0.6} \times 10^{34} I_{45}$  erg s $^{-1}$ , and conventional “magnetic field”,  $B = (3Ic^3 \dot{P} P / 8\pi^2 R^6)^{1/2} = 2.9_{-1.1}^{+0.8} \times 10^{12} I_{45}^{1/2} R_6^{-3}$  G, are typical for radio pulsars.

This result could be easily explained if one assumes that 1E 1207.4–5209 is merely a middle-aged field pulsar, unrelated to the SNR. If this pulsar were a background object at a distance well beyond the SNR, it would be difficult to explain the very high (thermal) X-ray luminosity — e.g.,  $L_x \approx 3 \times 10^{34}$  erg s $^{-1}$  at  $d = 10$  kpc cannot be emitted from radio pulsar polar caps because it exceeds  $\dot{E}$ , and it cannot be emitted from the surface of a cooling NS because the observed temperature is too high for such an age. One, however, might assume that the pulsar

is a foreground object, at a distance of several hundred parsecs, perhaps similar to the radio-quiet Geminga ( $\tau_c \sim 300$  kyr,  $d \sim 0.2$  kpc) or (radio-bright) PSR B1055–52 ( $\tau_c \sim 500$  kyr,  $d \sim 1$  kpc). In this case, the observed thermal-like pulsed X-ray radiation could be interpreted as emitted from hot polar caps with a size of a few hundred meters. The lack of detected radio and  $\gamma$ -ray radiation might be due to unfavorable orientation of pulsar beams (albeit  $\gamma$ -ray beams are expected to be rather broad). To explain the lack of softer thermal radiation from the entire cooling NS surface (like that observed from Geminga and PSR B1055–52), one could speculate that 1E 1207.4–5209 is older than the above-mentioned pulsars (e.g.,  $\tau_c \sim 1$  Myr cannot be ruled out), so that its surface temperature is lower, and its thermal radiation is too soft to be observable in X-rays. However, although the observed properties of 1E 1207.4–5209 cannot exclude the hypothesis that it is a foreground pulsar, the probability to find a middle-aged pulsar so close to the line of sight towards the SNR center is very low. Therefore, we consider this interpretation unlikely.

If 1E 1207.4–5209 is indeed associated with the SNR, we can reconcile the pulsar’s age with that of the SNR, assuming that the braking index  $n$  of the pulsar is large and/or its initial period  $P_0$  was close to its current value. If the pulsar slowdown is described by the equation  $\dot{f} = -Kf^n$ , then its age, for a constant  $K$ , is

$$\tau = \frac{P}{(n-1)\dot{P}} \left[ 1 - \left( \frac{P_0}{P} \right)^{n-1} \right]. \quad (2)$$

To obtain  $\tau \sim 20$  kyr (an upper limit on the age of PKS 1209–51/52), one can assume, for instance,  $n \sim 20$ –90 at  $P_0 \ll P$ , or  $P_0 \simeq 395$ –417 ms for  $n = 2.5$ . We are not aware of physical models of pulsar deceleration which would give so large braking indices, although Johnston & Galloway (1999) argue that empirical braking indices of relatively old pulsars can be as large as 20–50. On the other hand, there is no physical limitations on the initial period — it can be very close to its current value if the constant  $K$  in the slowdown equation is small.

It should be noted that 1E 1207.4–5209 is not the only pulsar that shows a characteristic age much older than the age of the SNR with which it is apparently associated. A similar example is the 7-s Anomalous X-ray Pulsar (AXP) 1E 2259+586 associated with the SNR CTB 109 — the SNR age,  $\sim 3$ –21 kyr (Rho & Petre 1997; Parmar et al. 1998), is much younger than  $\tau_c \simeq 226$  kyr (Kaspi, Chakrabarty, & Steinberger 1999). Another example is the 65 ms rotation-powered X-ray pulsar AX J1811.5–1926, whose period and period derivative were measured with ASCA (Torii et al. 1997, 1999), and association with the remnant G11.2–0.3 of the historic supernova A.D. 386 was strongly supported by *Chandra* observations (Kaspi et al. 2001a). The characteristic age of AX J1811.5–1926, about 24 kyr, is 15 times the true age.

If the pulsar was born in the supernova explosion that created PKS 1209–51/52, its X-ray luminosity,  $L_x \approx 1 \times 10^{33}$  erg s $^{-1}$  in the 0.5–6.0 keV band (at  $d = 2$  kpc), is 0.06–0.3 of the spin-down luminosity  $\dot{E}$ . This means that 1E 1207.4–5209 is different from AXPs, which show  $L_x > \dot{E}$ . On the other hand, the fraction of the spin-down luminosity detected in X-rays is too large to interpret the X-ray radiation as a nonthermal radiation or thermal polar-cap radiation emitted from a rotation-powered pulsar (in fact, the X-ray spectrum of 1E 1207.4–5209 is inconsistent with a nonthermal, power-law model — see Zavlin et al. 1998). Therefore, the original interpretation of the spectrum

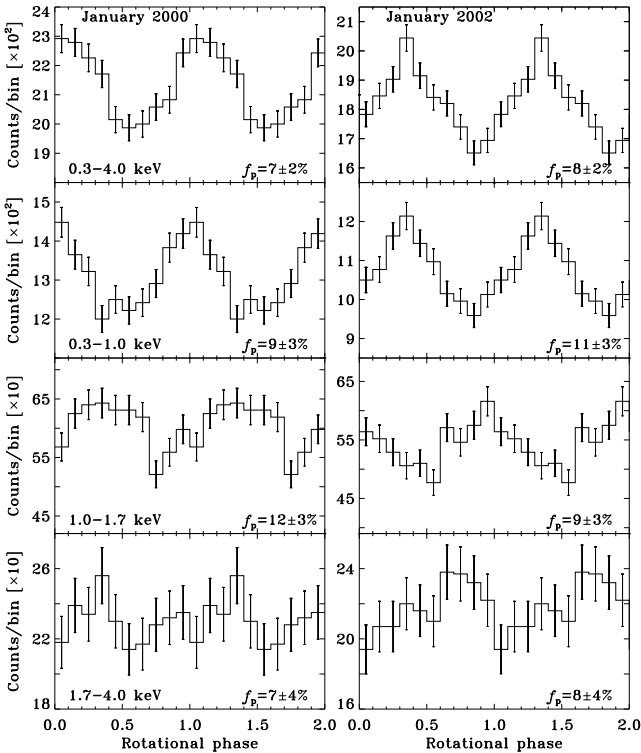


FIG. 3.— Light curves extracted in different energy ranges for the first and second observations (periods 0.4241296 s and 0.42413093 s, respectively).

as emitted from the surface of a cooling NS (Matsui, Long, & Tuohy 1988) remains most plausible, and the size of the emitting region and the effective temperature can be reconciled with those expected for a 10-kyr NS assuming that the NS is covered with a hydrogen or helium atmosphere (Zavlin et al. 1998). The magnetic field  $\sim 3 \times 10^{12}$  G, inferred from the estimated  $\dot{P}$  assuming a centered magnetic dipole and  $R_{\text{NS}} = 10$  km, may look too low to cause the temperature non-uniformity (Shibanov & Yakovlev 1996) required to explain pulsations detected from 1E 1207.4–5209. However, we can speculate that the magnetic dipole is off-centered, which can give a much stronger local magnetic field at the same value of the magnetic moment.

While estimating the period derivative from just two observations, one should not forget that such an estimate implies a lack of glitches or other timing irregularities. Young and middle-aged radio pulsars show glitches with  $\delta f$  up to  $5 \times 10^{-6} f$  (Lyne & Graham-Smith 1998). Even higher timing irregularities have been observed from some AXPs (e.g.,  $\delta f \sim 10^{-4} f$  in 1E 1048.1–5937 — Kaspi et al. 2001b). If, for instance, our pulsar had a glitch  $\delta f \sim 10^{-5} f$  just before the second observation, the pre-glitch frequency would be lower than the measured one by  $\sim 20 \mu\text{Hz}$ , which would increase the frequency shift and lowered the NS age by a factor of 3. Finally, we cannot rule out that 1E 1207.4–5209 is in a binary system with a long orbital period — our X-ray observations, each spanning about 8 hours, suggest that the period should be  $P_{\text{orb}} \gtrsim 40$  hours, as no effect of the binary orbit is clearly observed in the data, and the optical observations were not deep enough to exclude the presence of a faint secondary companion. In this case, the X-ray observations give Doppler-shifted periods — e.g., a radial velocity of  $10 \text{ km s}^{-1}$  corresponds to a shift of  $79 \mu\text{Hz}$ , much larger than the observed one. Therefore, the above estimates of pulsar parameters should be taken with caution until more timing observations of the pulsar are carried out.

To conclude, we measured the shift of the pulsar period between two *Chandra* observations. The period and its apparent derivative do not contradict to the hypothesis that it is a young pulsar physically associated with the SNR PKS 1209–51/52. From the data available, we cannot completely rule out that that this is a foreground middle-aged pulsar, but this alternative interpretation looks less plausible. The inferred properties of the pulsar warrant deep radio, optical, and  $\gamma$ -ray observations of this object. To understand the nature of the pulsar, its timing behavior should be monitored in X-rays, which would allow one to find out whether it shows strong timing irregularities or it is in a binary system. Another clue to the nature of 1E 1207.4–5209 would be provided by deep, high-resolution spectral observations of this object in X-rays, which could detect and identify spectral lines and evaluate the surface magnetic field of the neutron star.

We thank Glenn Allen and Allyn Tennant for the helpful advice on the ACIS timing issues. We are grateful to Marcus Teter and Fernando Camilo for useful discussions. This work was partly supported by SAO grant GO2-3088X and NASA grant NAG5-10865.

## REFERENCES

- Gregory, P. C., & Lored, T. J. 1996, *ApJ*, 473, 1059 (GL)  
 Helfand, D. J., & Becker, R. H. 1984, *Nature*, 307, 215  
 Johnston, S., & Galloway, D. 1999, *MNRAS*, 306, L50  
 Kaspi, V. M., Chakrabarty, D., & Steinberger, J. 1999, *ApJ*, 525, L33  
 Kaspi, V. M., Roberts, M. E., Vasisht, G., Gotthelf, E. V., Pivovarov, M., & Kawai, N. 2001a, *ApJ*, 560, 371  
 Kaspi, V. M., Gavriil, F. P., Chakrabarty, D., Lackey, J. R., & Munro, M. P. 2001b, *ApJ*, 558, 253  
 Lyne, A. G., & Graham-Smith, F. 1998, *Pulsar Astronomy* (New York : Cambridge University Press)  
 Matsui Y., Long K. S., Tuohy I. R. 1988, *ApJ* 329, 838  
 Mereghetti, S., Bignami, G. F., & Caraveo, P. A. 1996, *ApJ* 464, 842  
 Ögelman, H. 1995, in *The Lives of the Neutron Stars*, ed. M. A. Alpar, Ü. Kiziloglu, & J. van Paradijs (Kluwer: Dordrecht), p.101  
 Parmar, A. N., et al. 1998, *A&A*, 330, 175  
 Pavlov, G. G., Sanwal, D., Garmire, G. P., & Zavlin, V. E. 2002, in *ASP Conf. Ser. Neutron Stars in Supernova Remnants*, ed. P. O. Slane & B. M. Gaensler, in press (astro-ph/0112322)  
 Rho, J., & Petre, R. 1997, *ApJ*, 484, 828  
 Roger, R. S., Milne, D. K., Kesteven, M. J., Wellington, K. J., & Haynes, R. F. 1988, *ApJ*, 332, 940  
 Shibanov, Yu. A., & Yakovlev, D. G. 1996, *A&A*, 309, 171  
 Torii, K., Tsunemi, H., Dotani, T., & Mitsuda, K. 1997, *ApJ*, 489, L145  
 Torii, K., et al. 1999, *ApJ*, 523, L69  
 Vasisht, G., Kulkarni, S. R., Anderson, S. B., Hamilton, T. T., Kawai, N. 1997, *ApJ*, 476, L43  
 Zavlin, V. E., Pavlov, G. G., & Trümper, J. 1998, *A&A*, 331, 821  
 Zavlin, V. E., Pavlov, G. G., Sanwal, D., & Trümper, J. 2000, *ApJ*, 540, L25 (Paper I)